Cell

Mechanosensitive Hair Cell-like Cells from Embryonic and Induced Pluripotent Stem Cells

Kazuo Oshima,[1,2] Kunyoo Shin,[1,2] Marc Diensthuber,[1,2,3] Anthony W. Peng,[1,2] Anthony J. Ricci,[1,2] and Stefan Heller[1,2,*]
[1]Department of Otolaryngology—Head and Neck Surgery
[2]Department of Molecular and Cellular Physiology
Stanford University School of Medicine, Stanford, CA 94305
[3]Present address: Department of Otolaryngology—Head and Neck Surgery, Goethe University Medical School, 60590 Frankfurt am Main, Germany
*Correspondence: hellers@stanford.edu
DOI 10.1016/j.cell.2010.03.035

SUMMARY

Mechanosensitive sensory hair cells are the linchpin of our senses of hearing and balance. The inability of the mammalian inner ear to regenerate lost hair cells is the major reason for the permanence of hearing loss and certain balance disorders. Here, we present a stepwise guidance protocol starting with mouse embryonic stem and induced pluripotent stem cells, which were directed toward becoming ectoderm capable of responding to otic-inducing growth factors. The resulting otic progenitor cells were subjected to varying differentiation conditions, one of which promoted the organization of the cells into epithelial clusters displaying hair cell-like cells with stereociliary bundles. Bundle-bearing cells in these clusters responded to mechanical stimulation with currents that were reminiscent of immature hair cell transduction currents.

INTRODUCTION

Our inner ear harbors about 15,000 cochlear and about the same number of vestibular sensory hair cells, which are the mechanoreceptors of our senses of hearing and balance. Because of their paucity, molecular studies on hair cells have been limited, and, consequently, the inner ear shelters the last of our senses for which the molecular basis is unknown. Aside from being scarce, hair cells are also sensitive to mechanical and chemical insults. Acoustical overstimulation, chemotherapy, aminoglycoside drug side effects, the effects of aging, and increasingly noisy environments contribute to the deterioration of hearing over time. As a result, hundreds of millions of patients worldwide are permanently debilitated by hearing loss and balance problems. The main reason for the permanence of these chronic disorders is the fact that mammalian cochlear hair cells do not spontaneously regenerate and that the limited regeneration observed in the vestibular system is inadequate to restore function (Forge et al., 1993; Warchol et al., 1993).

Probably the most suitable renewable source for the generation of sensory hair cells are pluripotent stem cells, such as embryonic stem cells (ESCs) and induced pluripotent stem cells (iPSCs) (Beisel et al., 2008; Brigande and Heller, 2009). Whereas detailed and efficient protocols for the stepwise differentiation of retinal photoreceptors exist (Ikeda et al., 2005; Lamba et al., 2006; Osakada et al., 2008), only a single labor-intensive and protracted protocol has been devised for the generation of hair cell-like cells from mouse ESCs (Li et al., 2003). In all of these previous approaches, stem cell-generated retinal photoreceptor and hair cell-like cells were mainly defined by the expression of multiple marker proteins. However, a recent report shows that transplanted ESC-derived retinal cells restored light responses in a blind mouse model, indicating that the stem cell-generated photoreceptors can be functional when the progenitor cells are maturing in an enabling environment (Lamba et al., 2009).

The main goal of our study was to employ principles of early embryonic development and otic induction to generate a population of otic progenitor cells capable of differentiating into mechanosensitive sensory hair cells in vitro. ESCs and iPSCs isolated from an identical murine model were used in parallel to show that both pluripotent cell types differentiate along the otic lineage without major differences. We searched for conditions that promoted the differentiation of otic progenitors into hair cell-like cells that expressed a battery of marker genes and displayed protrusions that are highly reminiscent of stereociliary hair bundles. Finally, we were able to show that ESC- and iPSC-generated hair cell-like cells were responsive to mechanical stimulation and that these responses displayed transduction currents and adaptation reminiscent of immature hair cells.

RESULTS

ESCs and iPSCs from Math1/nGFP Mice

The transgenic mouse strain Math1/nGFP expresses a nuclear variant of enhanced green fluorescent protein (nGFP) that is driven by an *Atoh1* enhancer (Lumpkin et al., 2003). All sensory hair cells of the Math1/nGFP inner ear express nGFP from the time when they differentiate into nascent hair cells until adulthood (Figures S1A and S1B available online), which makes

stem cells isolated from this mouse line useful for guidance studies because stem cell-derived hair cell-like cells can be identified by nGFP expression (Diensthuber et al., 2009; Oshima et al., 2007). From Math1/nGFP blastocysts, we isolated four lines of ESCs that expressed typical ESC markers and displayed ESC colony morphology when grown on mouse embryonic fibroblast (MEF) feeders in the presence of leukemia inhibitory factor (LIF) (Figures S1C–S1G). Interestingly, all four Math1/nGFP ESC lines expressed the nGFP reporter, which was not unexpected because Math1 expression has been previously reported in ESCs (Azuara et al., 2006).

To generate iPSC lines, we infected Math1/nGFP embryonic fibroblasts with retroviruses expressing Oct4, Sox2, Klf4, and cMyc (Takahashi and Yamanaka, 2006). Primary colonies were picked, subcloned, and expanded on MEF feeder cells (Figure S2A). The iPSC lines expressed typical ESC marker genes as well as the Math1/nGFP reporter (Figures S2B and S2C).

We randomly differentiated ESC and iPSC lines by generation of embryoid bodies, removal of LIF, and culturing the embryoid body cells before analyzing expression of endo-, meso-, and ectodermal markers. We found upregulation of transcripts for GATA6, Brachyury, and microtubule-associated protein 2 (MAP2), which was confirmed by immunocytochemistry (Figures S3A–S3F). In differentiated cell populations, expression of the nGFP reporter was reduced or absent, and cells that expressed germline-specific markers were consistently nGFP negative. This observation indicates that the Math1/nGFP reporter is active in ESCs and iPSCs and downregulated upon differentiation of the cells. When ESC and iPSC lines were injected subcutaneously into immunodeficient mice, we found formation of typical teratomas. The teratomas consisted of tissues that could be assigned to all three germ layers, indicative of the pluripotency of the ESC and iPSC lines (Figure S4).

Generation of Presumptive Ectoderm that Is Competent to Otic Induction

It has been hypothesized that inhibition of primitive streak cell identities during embryoid body formation will suppress the induction of endo- and mesoderm from uncommitted epiblast cells. Establishment of primitive streak cells upon differentiation of ESCs depends on the presence of active Wnt and TGF-β/nodal/activin signaling, which recapitulates early events that lead to germ-layer induction in the mammalian embryo (Gadue et al., 2006). We anticipated that interference with Wnt and TGF-β signaling would strongly suppress the formation of primitive streak cells and concomitantly increase presumptive ectoderm. In addition, we presumed that activation of IGF signaling would promote the formation of anterior ectoderm (Pera et al., 2001), which is more competent to otic induction than trunk ectoderm (Groves and Bronner-Fraser, 2000). Similar strategies were used to generate ectoderm that is capable of differentiating into retinal cell types (Ikeda et al., 2005; Lamba et al., 2006; Osakada et al., 2008).

Embryoid bodies, generated from ESCs and iPSCs, were treated with the Wnt inhibitor Dkk1 (Glinka et al., 1998), the selective inhibitor of Smad3 (SIS3) that interferes with TGF-β signaling (Jinnin et al., 2006), and IGF-1, either alone or in combinations (Figure 1A). Embryoid body-derived cells were attached to culture dishes and stained with antibodies to Brachyury and GATA6, indicators of differentiation along the meso- and endodermal lineages, respectively. We observed that treatment of ESC-derived embryoid bodies with either Dkk1 or SIS3 alone significantly reduced the number of Brachyury-positive cells (Figure 1B). For iPSC-derived embryoid bodies, only Dkk1 alone was able to significantly reduce the Brachyury-expressing cell population (Figure 1C). Combination of Dkk1 and SIS3 significantly reduced the number of Brachyury-positive cells from 65.0% ± 14.9% to 20.9% ± 6.9% in ESC-derived populations and from 44.1% ± 9.6% to 15.3% ± 6.5% in iPSC-derived populations (Figures 1B and 1C). These two factors also led to significant reduction of the GATA6-positive cell population from 24.9% ± 3.1% to 10.1% ± 3.7% (ESC derivatives) and from 34.3% ± 7.1% to 13.9% ± 8.4% (iPSC derivatives). Combination of Dkk1, SIS3, and IGF-1 (D/S/I) was most effective, leading to a reduction of Brachyury-positive cells to 20.8% ± 13.1% and of the GATA6-expressing cell population to 9.8% ± 5.0% in ESC-derived cell populations (Figures 1B and 1D). Likewise, iPSC-derivatives displayed reduction to 14.3% ± 5.8% (Brachyury) and 12.1% ± 6.8% (GATA6) (Figures 1C and 1E). The reduction of Brachyury and GATA6 expression was also detectable at the transcript level, where the mRNA for the ESC marker Nanog was also reduced most in D/S/I-treated cultures (Figures 1F and 1G).

To test for competence to otic induction, we plated the D/S/I-treated embryoid bodies into gelatin-coated culture dishes and exposed them to FGFs, which have been shown to be both sufficient and necessary for otic induction (Freter et al., 2008; Ladher et al., 2005; Phillips et al., 2004; Pirvola et al., 2000; Pirvola et al., 2002). We used bFGF as a general otic inducer because it activates several different FGF receptor subtypes and has been previously used to substitute for the proposed natural otic-inducing FGF3 and FGF10 (Groves and Bronner-Fraser, 2000; Pauley et al., 2003; Vendrell et al., 2000; Wright and Mansour, 2003). As a marker for otic induction, we used antibodies to Pax2 (Li et al., 2004), and we quantified the number of Pax2-positive cells after 3 day treatment with bFGF (Figure 2A). In both ESC- and iPSC-derived populations, we observed the largest increase of Pax2-positive cells in cultures that were previously exposed to D/S/I, reaching 29.8% ± 7.1% for ESC derivatives and 19.6% ± 5.6% for iPSC derivatives (Figures 2B–2E). Comparable results were obtained when we used FGF3 and FGF10 instead of bFGF, which resulted in 24.6% ± 4.0% Pax2-positive cells for ESC derivatives and 16.3% ± 4.0% for iPSC derivatives (n = 3). Neither the initial factors alone nor combinations of two factors were as effective as the triple combination; therefore all three factors/compounds are needed to generate a cell population that is most responsive to FGF treatment. Dkk1 and SIS3 are mainly effective in suppressing endo- and mesodermal lineages, whereas the effect of IGF-1 only became obvious after FGF induction, where D/S/I-treatment resulted in an increased number of Pax2-positive cells when compared with D/S treatment (p values [paired t test] for these experiments were 0.04 for ESC-derived cells and 0.1 for iPSC-derived cells indicative of significance in case of ESC-derived cells and a possible trend for iPSC-derived cells) (Figures 2B and 2C). Control cultures not treated with any of the

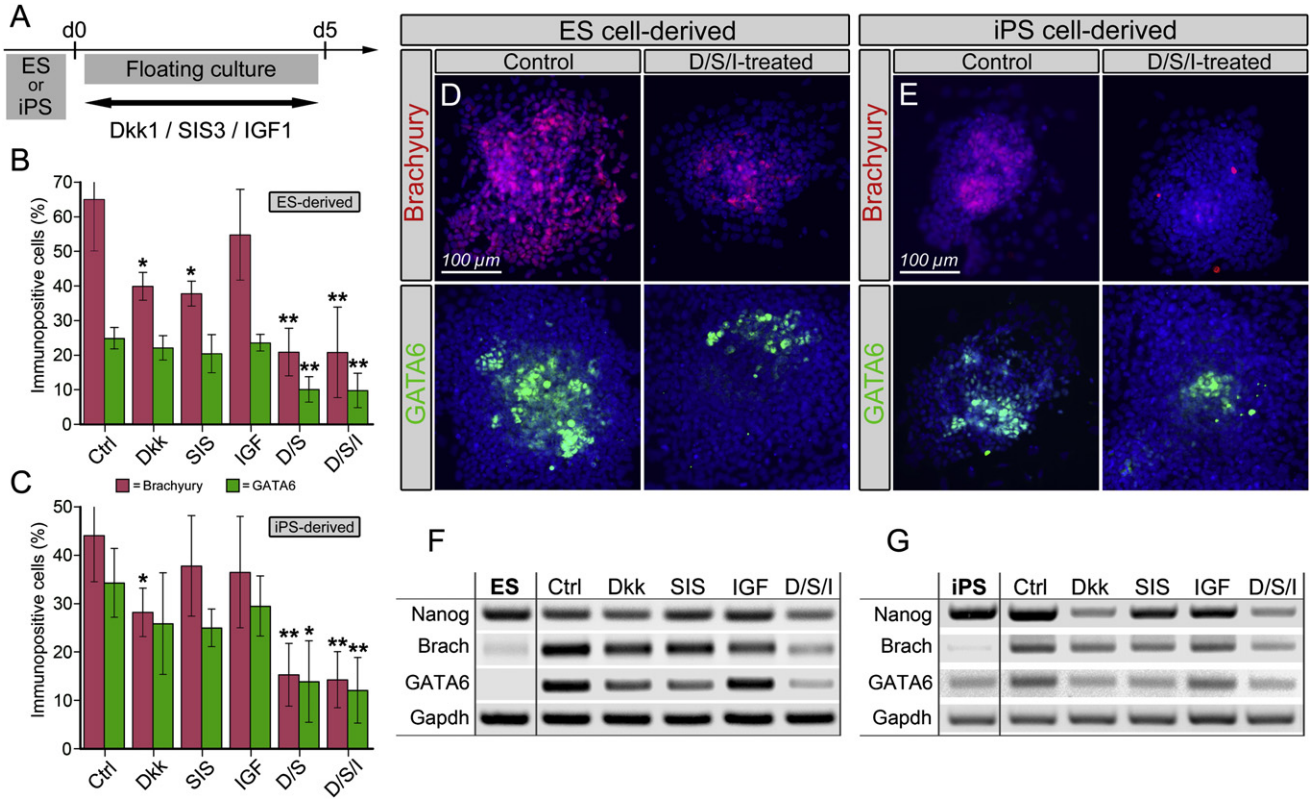

Figure 1. Suppression of Meso- and Endodermal Cell Differentiation by Interference with Wnt- and TGF-β Signaling

(A) C9 ESCs and No.25-5 iPSCs were dissociated into single cells and cultured in nonadhesive plates for 5 days to form embryoid bodies in presence of Dkk1, SIS3, and IGF-1, as indicated.

(B and C) Embryoid bodies from ESCs (B) and iPSCs (C) were generated in presence of the factors indicated. Ctrl, no factors added; D/S, Dkk1 and SIS3; D/S/I, Dkk1, SIS3, and IGF-1. Error bars represent the SD. n = 5. * indicates $p < 0.05$ and ** indicates $p < 0.01$, determined with paired, two-tailed t tests.

(D and E) Representative immunostainings of plated embryoid bodies from ESCs (D) and iPSCs (E). Treatment with D/S/I reduced the number of cells immunopositive for Brachyury and GATA6.

(F and G) RT-PCR analyses show downregulation of transcripts for Brachyury and GATA6 in D/S/I-treated cultures of ESC- (F) and iPSC- (G) derived populations. Expression of the pluripotent and ESC marker Nanog is also reduced most noticeably after D/S/I treatment. Ctrl, embryoid bodies generated without factors added; ES, ESCs before differentiation; iPS, iPSCs before differentiation.

Nuclear DAPI staining is shown in blue. See also Figures S1, S2, S3, and S4.

three initial factors, but treated with bFGF, displayed only a few Pax2-expressing cells (0.05 ± 0.04% for ESC and 0.1 ± 0.09% for iPSC derivatives).

RT-PCR confirmed the strong upregulation of Pax2 in ESC and iPSC cultures after D/S/I treatment and exposure to bFGF (Figures 2F and 2G). Transcripts for other genes that are expressed in the developing inner ear, such as Pax8, Dlx5, Six1, and Eya1 (Brown et al., 2005; Groves and Bronner-Fraser, 2000; Ohyama et al., 2006; Xu et al., 1999; Zou et al., 2004), were also most abundant in D/S/I- and bFGF-treated cultures. Double immunostaining revealed that 56.0% ± 5.3% of the Pax2-positive cells in ESC-derived cultures coexpressed the otic marker Dlx5 (Figure 2H). Conversely, 73.2% ± 10.3% of Dlx5-positive cells coexpressed Pax2. In the native developing inner ear, Pax2 expression precedes Dlx5 expression (Brown et al., 2005), and it is therefore not surprising to find only partial coexpression. Likewise, 64.1% ± 5.6% of Pax2-expressing cells colabeled with antibody to Pax8 (Figure 2I); 43.0% ± 8.3% of Pax8-positive cells coexpressed Pax2. Pax8 is induced prior to Pax2 in the native developing inner ear (Hans et al., 2004; Heller and Brändli, 1999) and well before Dlx5; therefore, we did not expect to detect complete coexpression of these markers because their temporal expression periods during native otic development do not completely overlap.

Pax2 is not an inner ear-specific marker. For example, it is also expressed in neural progenitors in close vicinity to the otic vesicle at the midbrain/hindbrain boundary, where it is coexpressed with engrailed 1 (Rowitch and McMahon, 1995) (Figure S5A). Engrailed 1, however, is not associated with Pax2-expressing otic progenitor cells in the developing otic vesicle (Figures S5A and S5B). D/S/I+bFGF treatment only resulted in 1.2% ± 0.8% of engrailed 1-positive cells, which all expressed Pax2, indicating that the vast majority of Pax2-positive cells were not midbrain/hindbrain boundary neural progenitors.

Our guidance strategy utilizes similar steps as retinal cell guidance protocols (Ikeda et al., 2005; Lamba et al., 2006; Osakada et al., 2008). As a result, we would expect to find retinal progenitors in ESC- and iPSC-derived cultures. Indeed, Pax6-expressing

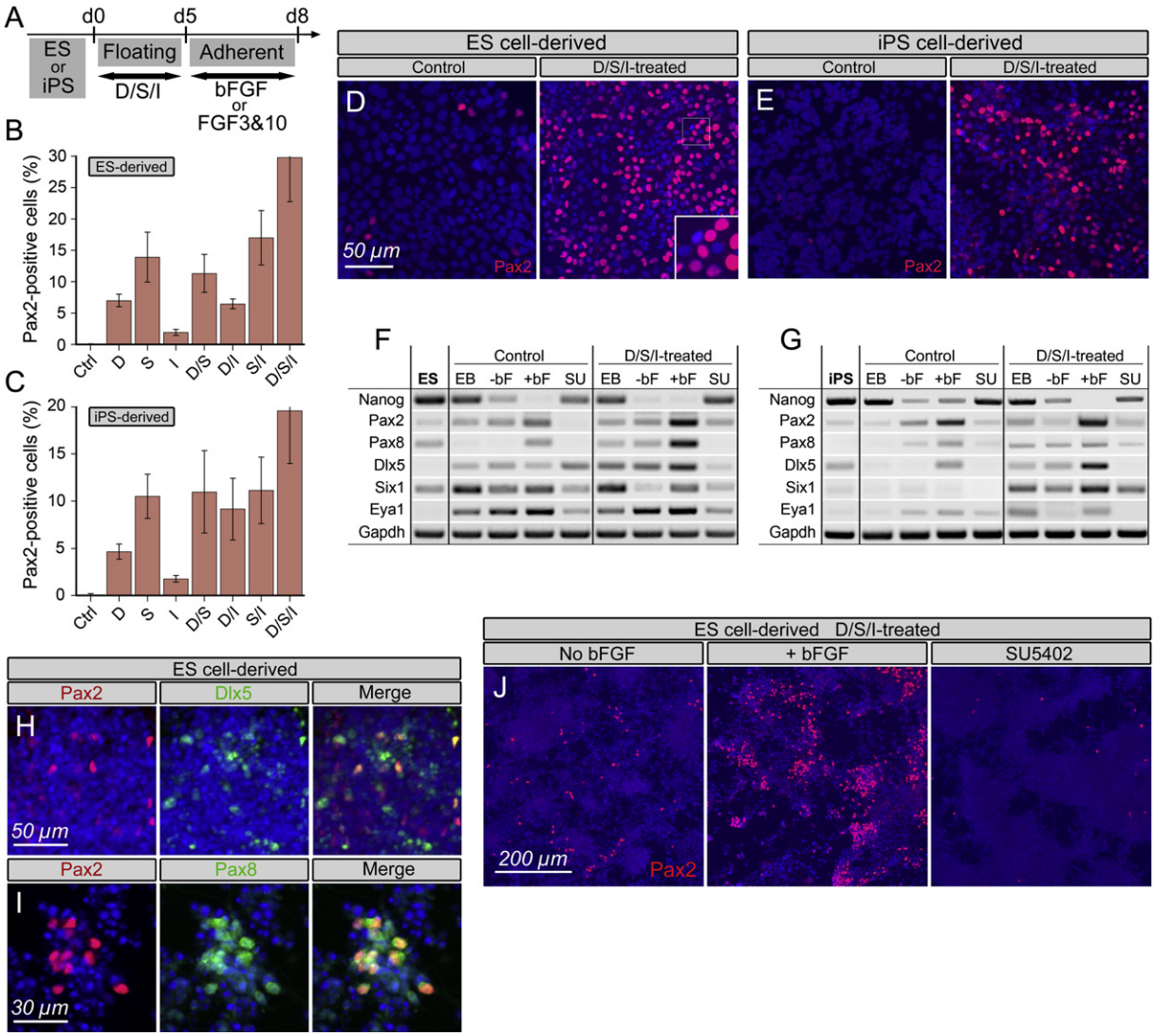

Figure 2. Otic Induction Is Most Efficient in D/S/I-Treated ESCs and iPSCs

(A) Embryoid bodies were generated for 5 days in presence of of Dkk1, SIS3, and IGF-1, as indicated; subsequent adherent culture was done for 3 days in fibronectin-coated plates in presence of otic inducers bFGF or FGF3&10.

(B and C) ESC- (B) and iPSC- (C) derived cultures, exposed for 3 days to bFGF, were immunostained with antibodies to Pax2, and the percentage of Pax2-positive cells of the total cell population was determined. D/S/I treatment most efficiently increased the number of cells that responded with upregulation of Pax2 to bFGF-treatment. Ctrl, no added factors during embryoid body formation. Error bars represent the SD. n = 3.

(D and E) Representative immunocytochemical images showing upregulation of Pax2 in ESC-derived (D) and iPSC-derived (E) cultures in response to D/S/I treatment followed by bFGF exposure. Control, bFGF-treated cultures of embryoid bodies generated with no added factors. The inset shows a higher-magnification view of the nuclear staining.

(F and G) RT-PCR analyses for expression of Nanog and the early otic markers Pax2, Pax8, Dlx5, Six1, and Eya1 in cultures derived from ESCs (F) and iPSCs (G). ES, ESCs before differentiation; iPS, iPSCs before differentiation; EB, embryoid bodies harvested at day 5 (d5). −bF and +bF indicate absence and presence of bFGF between d5 and d8. SU, SU5402 treatment between d5 and d8.

(H and I) Coexpression of otic markers Pax2 and Dlx5 (H) and of Pax2 and Pax8 (I) in the majority of ESC-derived cultures after D/S/I and bFGF treatment.

(J) Cultures of D/S/I-treated ESC-derived embryoid body cells in absence and presence of bFGF as well as after treatment with SU5402, which virtually diminished Pax2 expression.

Nuclear DAPI staining is shown in blue. See also Figure S5.

cells were detectable in D/S/I+bFGF-treated cultures and were clearly distinct from the Pax2-positive cell population (Figure S5C).

Native otic induction is blocked by inhibition of FGF signaling (Alsina et al., 2004; Martin and Groves, 2006). Blockade of FGF signaling with the FGF receptor inhibitor SU5402 resulted in abolishment of Pax2 induction (Figure 2J), which shows that also in guidance experiments, FGF signaling is essential for otic induction from presumptive ectodermal cells. Overall, the

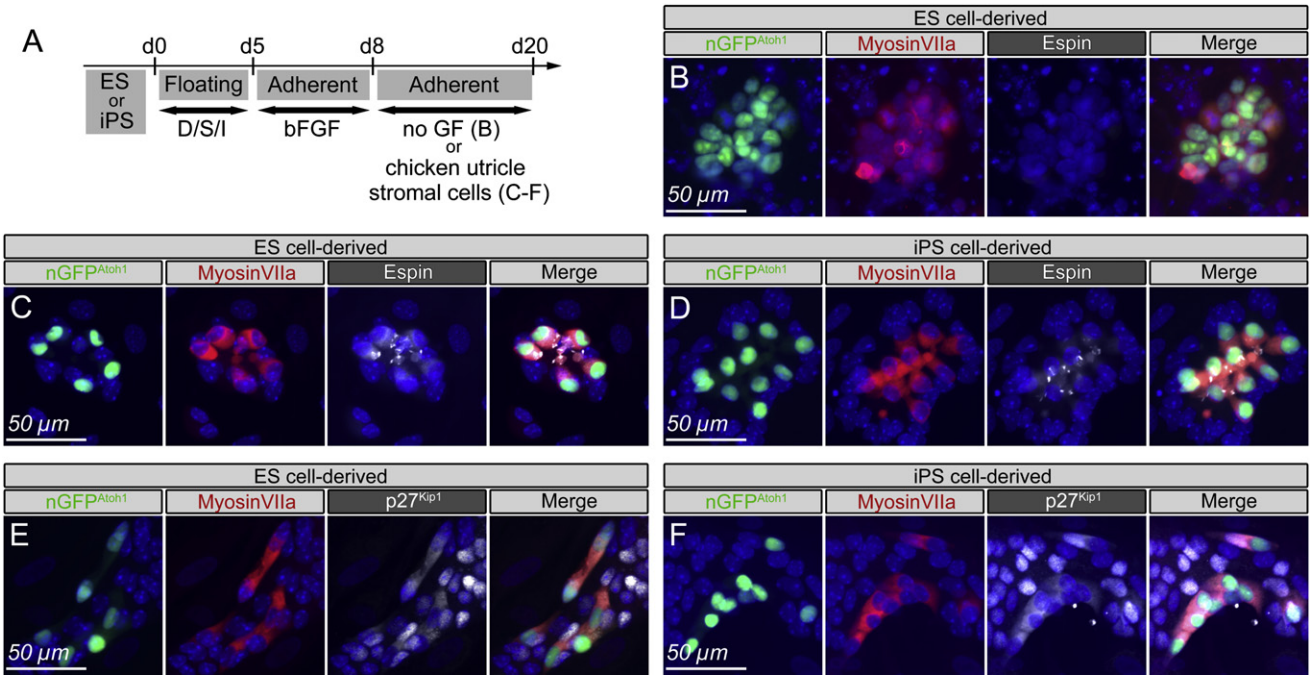

Figure 3. Differentiation into Hair Cell-like Cells

(A) ESCs or iPSCs were cultured in nonadherent condition in presence of Dkk1, SIS3, and IGF-1 (D/S/I) and the resulting embryoid bodies were grown adherently in presence of bFGF. On day 8 (d8), the cells were replated and kept for 12 days without adding additional growth factors (no GF), or maintained on mitotically inactivated chicken utricle stromal cells.

(B) When cells were cultured without added growth factors, we observed differentiation into nGFP^{Atoh1}-positive cells that were immunopositive for myosin VIIa but did not display expression of espin or other hair bundle markers.

(C and D) When the ESC- (C) and iPSC- (D) derived progenitors were cultured on chicken utricle stromal cells, we found nGFP^{Atoh1} and myosinVIIa double-positive cells that coexpressed the hair bundle marker espin.

(E and F) ESC- (E) and iPSC- (F) derived progenitors that expressed nGFP^{Atoh1} displayed cytosolic immunoreactivity for p27^{Kip1} and were surrounded by nGFP-negative cells with nuclear p27^{Kip1} expression.

Nuclear DAPI staining is shown in blue. See also Figure S6.

strong upregulation and coexpression of multiple early inner ear markers suggests that D/S/I followed by bFGF treatment sufficiently mimics, in a culture dish, the events leading to otic induction during normal embryonic development.

Hair Cell Differentiation

Withdrawal of growth factors and serum-free culture on gelatin is an effective way to initiate differentiation of ESC-generated otic progenitors (Li et al., 2003). This approach led to upregulation of hair cell markers, but in culture, the generated hair cell-like cells did not adopt typical hair cell morphology. We tested four different substrates for differentiation of ESC- and iPSC-generated otic progenitors, generated by D/S/I+bFGF treatment. When ESC- and iPSC-derived cells were plated onto fibronectin, gelatin, or MEF feeders, we detected nGFP-positive cells (Figures 3A and 3B). Per 10^4 plated cells, 955 ± 153, 857 ± 240, and 520 ± 95 nGFP-positive cells were found in ESC-derived cultures, as well as 670 ± 110, 597 ± 170, and 360 ± 66 nGFP-positive cells in iPSC-derived cultures (on fibronectin, gelatin, and MEFs, respectively; n = 3). A subpopulation of the nGFP-positive cells was immunopositive for the hair cell marker myosin VIIa: 37 ± 5, 12 ± 8, and 33 ± 12 (ESC derived) and 24 ± 6, 8 ± 5, 25 ± 6 (iPSC derived). We detected neither cytomorphological specializations nor expression of hair bundle markers, such as espin (Zheng et al., 2000).

When we plated the ESC- and iPSC-derived otic progenitors onto a layer of mitotically inactivated chicken utricle stromal cells, we observed a different behavior. The progenitors formed defined patches of cells that harbored nGFP-positive cells, which coexpressed the hair cell marker myosin VIIa and the actin filament-bundling protein espin (Figures 3C and 3D), which is abundantly expressed in the stereocilia of the mechanosensitive hair bundle, where it is necessary for hair cell function (Zheng et al., 2000). Per 10^4 plated cells, 1186 ± 150 (ESC derived) and 908 ± 209 (iPSC derived) cells were nGFP positive, 139 ± 49 and 113 ± 24 cells were nGFP and myosin VIIa positive, and 36 ± 7 and 24 ± 19 cells expressed both markers plus espin (n = 4). When we plated 10^4 control cells that were not subjected to D/S/I, but were otherwise treated identically, we only found a few (135 ± 84 and 30 ± 18, ESC and iPSC derived) nGFP-positive cells and no myosin VIIa- or espin-expressing cells (n = 4). These results show that D/S/I treatment is a specific requirement for hair cell differentiation from ESCs and iPSCs.

Interestingly, the cells surrounding the nascent hair cell-like cells displayed nuclear immunoreactivity for p27^{Kip1} (Figures 3E and 3F), a cell-cycle regulator that is initially expressed in the

nuclei of all cells of the prosensory domains of the developing inner ear and later becomes restricted to supporting cells (Chen and Segil, 1999). In nascent hair cells, $p27^{Kip1}$ translocates from the nucleus to the cytoplasm before the protein is no longer detectable in fully differentiated hair cells. We observed that after 12 days of differentiation culture, the majority of nGFP/myosin-VIIa double-positive cells displayed cytoplasmic $p27^{Kip1}$ immunoreactivity.

Supporting cells isolated and expanded from embryonic chicken utricle have previously been used to generate hair cell-like cells (Hu and Corwin, 2007). We performed a series of control experiments to ensure that hair cell-like cells that differentiated in ESC- and iPSC-derived cultures were neither chicken hair cells nor the product of fusion of a murine cell with a chicken hair cell. First, it is unlikely that chicken hair cells will develop from the nonsensory stromal cell layer. When we cultured inactivated chicken utricle stromal cells for up to 3 weeks, we never observed cells with hair cell morphology or cells that expressed hair cell markers (Figure S6A). Furthermore, ESC- and iPSC-derived myosin VIIa- and nGFP-positive cells did not stain with a monoclonal antibody specific to the chicken isoform of hair bundle protein tyrosine phosphatase receptor Q (Ptprq, also known as hair cell antigen [Goodyear et al., 2003]) (Figures S6B and S6C). Conversely, chicken hair cells, derived from dissociated otic vesicle cells that were seeded onto stromal cells, displayed strong Ptprq immunoreactivity but lacked nuclear green fluorescence (Figure S6D).

ESC- and iPSC-Derived Hair Cell-like Cells Have Stereociliary Hair Bundles

The occurrence of asymmetrically distributed espin immunoreactivity toward one side of the presumptive hair cells (Figures 3C and 3D) raised the question of whether the cells were developing hair bundle-like structures. To answer this question, we analyzed clusters containing nGFP-positive cells by scanning electron microscopy (SEM) (Figure S7). Protruding from the surface of the clusters, structures that were highly reminiscent of stereociliary hair bundles were visualized at different stages of maturation (Figures 4A–4C and 4H–4J) (Tilney et al., 1992). The hair bundle-like structures displayed single acentric protrusions reminiscent of kinocilia, which were consistently located toward the side of the bundle that featured the tallest stereocilia-like protrusions. Cytoskeletal stereocilia cores consist of F-actin, crosslinked by espin, whereas kinocilia are tubulin filled. When we visualized F-actin and espin in bundles protruding from ESC- and iPSC-derived clusters, we found that stereocilia-like extensions were labeled with phalloidin and antibody to espin (Figures 4D, 4E, and 4K–4L). The longer kinocilia remained unlabeled with both reagents, but they displayed immunoreactivity for tubulin (Figures 4F, 4G, 4M, and 4N).

We further noticed many interstereociliary links as well as links between the tips of stereocilia and the sides of taller neighboring stereocilia (Figures 5A–5C). Multiple links are reminiscent of nascent hair cells, which transiently display many interstereociliary links that can be visualized with antibodies to cadherin 23 (Boëda et al., 2002; Kazmierczak et al., 2007; Michel et al., 2005; Siemens et al., 2004). We found that the protrusions were labeled with antibodies to cadherin 23 (Figures 5E and 5F), further indicating that the bundles correspond to immature hair cell stereociliary bundles. The tops of short stereocilia that are connected with tip links to their taller neighbors usually appear to be pointed and asymmetric (Lin et al., 2005), which could be an indication of tension in the link. ESC- and iPSC-derived hair cell-like cells displayed asymmetric or pointed stereociliary tips that appeared to be linked by thin filaments to the sides of the next tallest neighbors (Figures 5B and 5C). Finally, we observed that stereocilia of stem cell-derived hair cell-like cells were tapered at their bases (Figure 5D), which is a hallmark of hair cell stereocilia (Tilney et al., 1983).

These results show that mitotically inactivated utricle stromal cells provide one or a combination of signals that induce the formation of hair bundles. Although the activity provided by stromal cells is unknown, we hypothesize that the signal(s) are not entirely secreted because stromal cell conditioned medium was unable to evoke hair bundle differentiation (no espin-positive cells, n = 3). Conversely, plating of ESC- and iPSC-derived cells on paraformaldehyde-fixed utricle stromal cells also resulted in abolishment of the hair bundle-inducing activity (n = 3). Future identification of these signals could provide important clues about the mechanisms controlling the initiation of hair bundle growth during embryonic development. Our results indicate that hair bundles only grow in cells that express Math1 and myosin VIIa, but that expression of Math1 and myosin VIIa is not sufficient to induce hair bundle formation.

ESC- and iPSC-Derived Hair Cell-like Cells Are Mechanosensitive

The occurrence of hair bundle-like structures with asymmetric tips and interstereociliary links raised our curiosity of whether the cells were responsive to mechanical stimulation. A total of 52 cells were successfully recorded, with 42 being derived from ESCs and ten being derived from iPSCs. No statistical differences were observed in any measured parameter. Cell capacitance was 3.7 ± 1.0 pF (n = 52) and series resistance was 14 ± 7 MΩ (n = 52) prior to compensation of up to 50%. Resting potentials were −45 ± 7 mV (n = 7). Mechanosensitivity was probed in 45 of these cells with 24 positive responses. Figure 6 shows examples of responses from both ESC- and iPSC-derived cells. The mean current amplitude was 74 ± 82 pA with responses ranging from 14 pA to 370 pA. Normalized current-displacement plots are shown in Figure 6E for ESCs (n = 5) and iPSCs (n = 6). Single Boltzmann functions of the form $I/I_{max} = 1/(1 + e^{-(x-x_0)/dx})$, where x_0 is the half activating displacement and dx is the slope, found no differences between populations. Values for x_0 of 198 ± 9 and 224 ± 18 nm and dx values of 125 ± 11 and 125 ± 18 nm^{-1} were obtained for ESC- and iPSC-derived cells, respectively.

Adaptation is a complex process in which hair bundle dynamic range is enhanced and sensitivity maintained over large displacements (Eatock, 2000). It likely involves multiple mechanisms and has several distinct temporal components in mature hair cells (Wu et al., 1999). Adaptation matures in a stepwise manner, so that immature cells show little adaptation while mature cells have robust adaptation (Lelli et al., 2009; Michalski et al., 2009; Waguespack et al., 2007). Our results show a broad

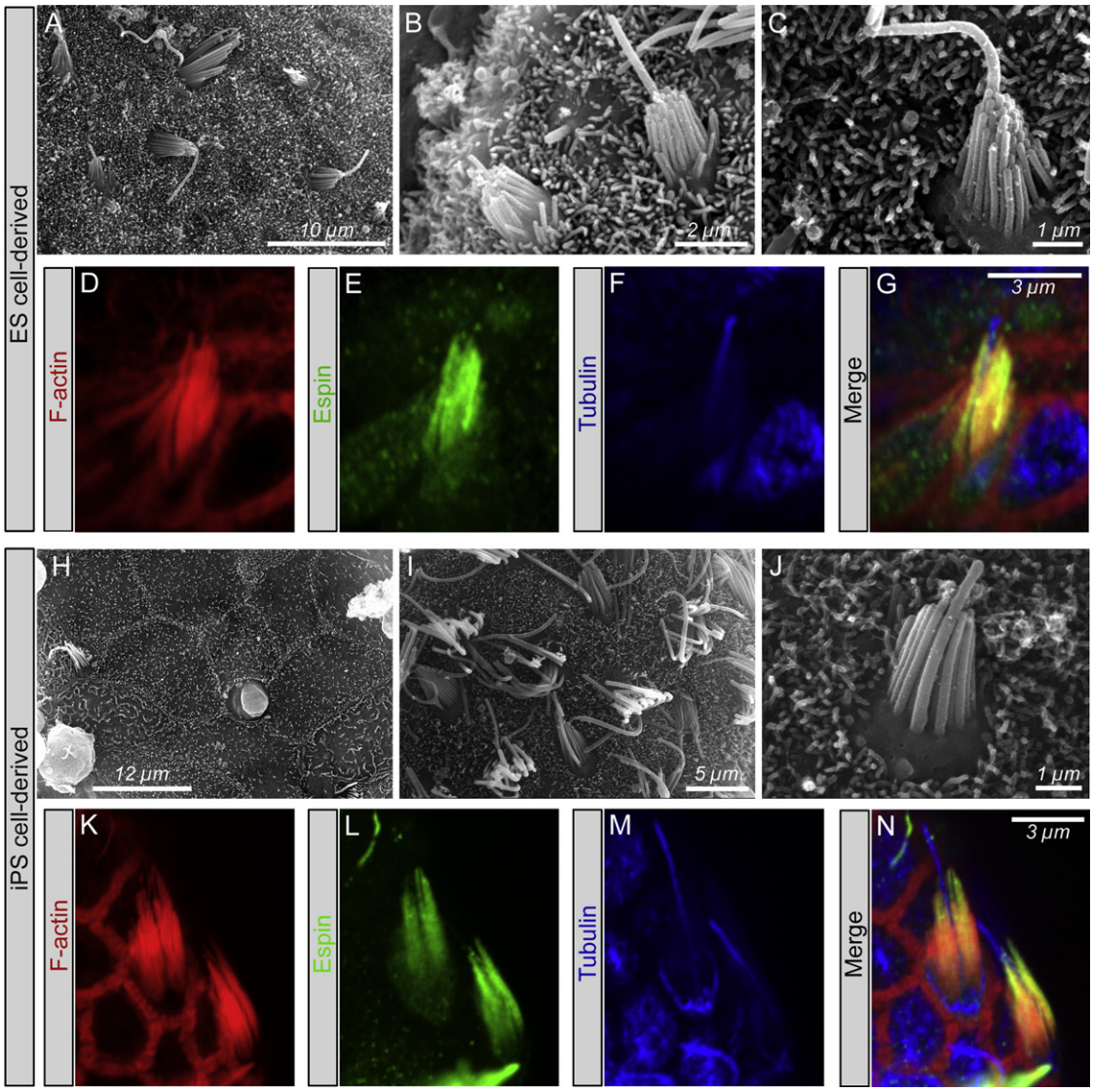

Figure 4. Hair Bundle-like Protrusions of ESC- and iPSC-Derived Cells

(A–C and H–J) Scanning electron microscopic views of the surface of ESC- (A–C) and iPSC- (H–J) derived cell clusters after 12 days differentiation on mitotically inactivated chicken utricle stromal cells.

(D–G and K–N) Projections of confocal stacks of hair bundle-like protrusions of ESC- (D–G) and iPSC- (K–N) derived cells. F-actin-filled membrane protrusions were visualized with TRITC-conjugated phalloidin (red). The actin-bundling stereociliary protein espin was visualized with FITC-conjugated secondary antibodies (green), and antibodies to beta-tubulin were visualized with Cy5-conjugated secondary antibodies to visualize the kinocilium-like structures (blue).

See also Figure S7.

range of responses. 18% of the cells showed no adaptation, 45% showed a single time constant for decay of the current, and 37% showed the more mature double exponential decay in currents (Figures 6D and 6F). The fast time constant measured was 0.5 ± 0.4 ms (n = 5) and the slow was 11 ± 5 ms (n = 5). No relationship to current amplitude was observed. Directional sensitivity also matures over time and appears to correlate with the alignment of tip links orienting in one direction along the stereocilia (Waguespack et al., 2007). Immature hair cells do not show directional sensitivity. In a population of cells tested here, directional sensitivity was also ambiguous, as shown in Figure 6G. This example demonstrates that either pushing or pulling on the hair bundle elicited an increase in current. Hair cell mechanotransduction currents are blocked by aminoglycosides (Kroese et al., 1989; Marcotti et al., 2005; Ricci, 2002). Mechanically induced currents were tested for pharmacologic sensitivity by local application of 1 mM dihydrostreptomycin (DHSM) to hair bundles and then mechanical stimulation. Both ESC- and iPSC-derived hair cell-like cell responses were antagonized reversibly by DHSM (Figures 6H and 6I), supporting the argument that the elicited current was comparable to that evoked in native sensory hair cells.

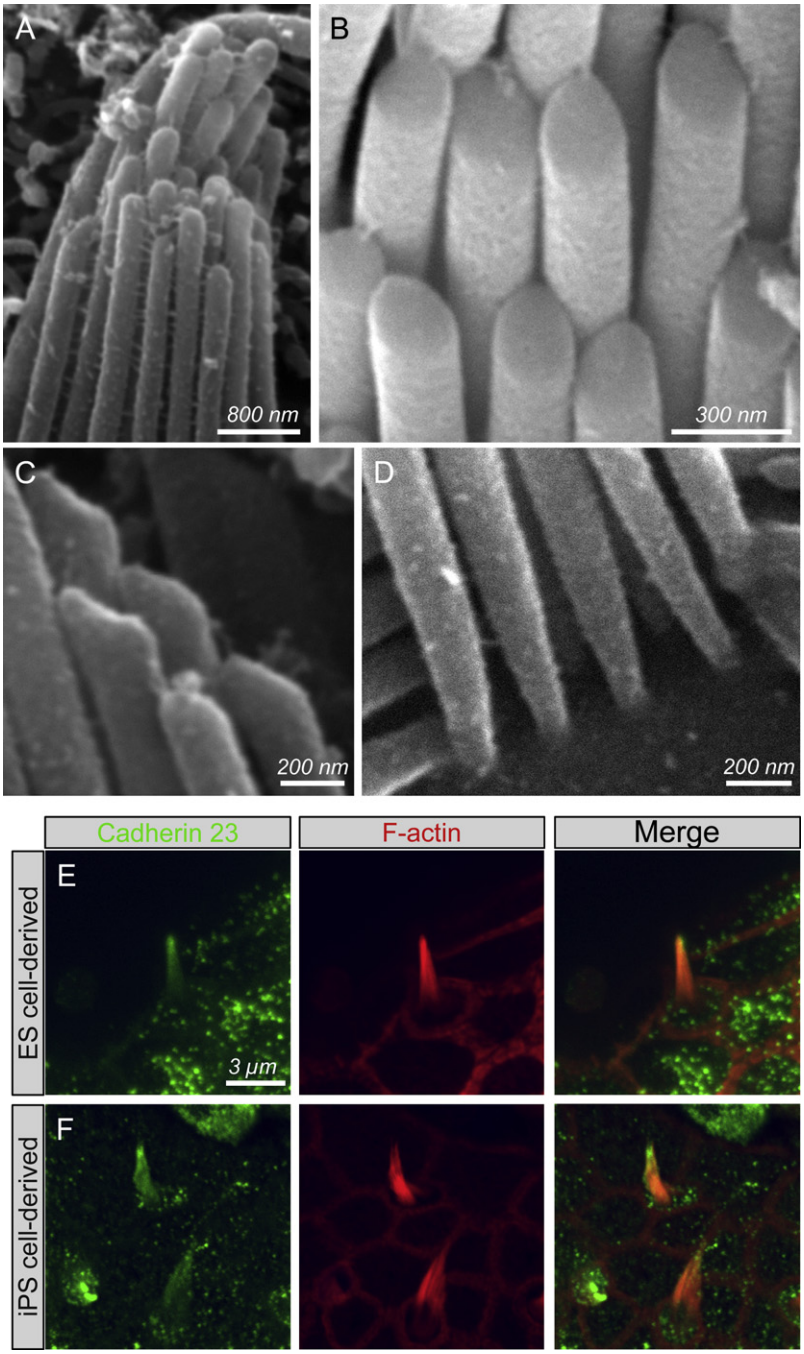

Figure 5. Hair Bundle-like Protrusions and Interstereociliary Links Revealed with Scanning Electron Microscopy and Expression of Cadherin 23

(A) Many links between stereociliary-like protrusions on a ESC-derived cell.

(B) An iPSC-derived cell shows stereociliary-like membrane protrusions that are connected at their tops with their taller neighbors. Also note the asymmetrical shape of the tops.

(C) Asymmetrical tops and connections in an ESC-derived cell.

(D) Tapered bases of stereociliary-like protrusions in an ESC-derived cell.

(E and F) Hair bundle-like protrusions of ESC- (E) and iPSC- (F) derived cells immunostained with antibodies to cadherin 23 (FITC, shown in green) and colabeled with TRITC-conjugated phalloidin (shown in red).

Hair Bundle-Bearing ESC- and iPSC-Derived Cells Display a Variety of Voltage-Dependent Currents

Voltage-dependent currents were also investigated in the same group of cells. Again, no differences between ESC- and iPSC-derived cells were observed. A great deal of diversity was observed in the cell responses measured. Figure 7 shows representative examples of the types of responses observed. Current magnitudes with K^+ as the major intracellular ion ranged from 397 pA to 4982 pA with a mean of 2190 ± 1595 pA (n = 24). Cells shown in Figure 7A are distinguished by the presence of an inward current, likely Na^+, where ten out of 30 cells tested were positive for this current. Figure 7C shows an expanded view of the initial current response for a cell with an inward current. Additionally, two major types of outward currents were observed, those that activated rapidly and showed some level of inactivation and those that activated more slowly with little inactivation. The predominant response was a slowly activating, noninactivating conductance with no inward current. Most cells showed components of each to different degrees. Steady-state activation properties also varied considerably with half activating voltages ranging from −17 mV to 23 mV with the more negative activation associated with the inactivating currents, and the more depolarized with the more slowly activating, noninactivating currents. Experiments with Cs^+ replacing K^+ revealed two kinetically distinct components that were carried by Cs^+ (Figure 7B). About half of the cells had a rapidly activating component, while about 20% had a more slowly activating current, and 30% had no Cs^+-permeant component at all.

DISCUSSION

In this study, we utilized principles of early development to suppress the differentiation of ESCs and iPSCs along endo- and mesodermal lineages. The resulting presumptive ectoderm displayed competence to respond to otic-inducing FGFs. The generated otic progenitor cells were capable of differentiation into hair cell marker-expressing cells, independent of the substrate they were cultured on. The development of cytomorphological specializations, such as hair bundle-like protrusions, however, required coculture with fibroblast-like cells that were isolated from embryonic chicken utricles after removal of the sensory epithelial layers. In these cultures, the hair cell-like cells were organized

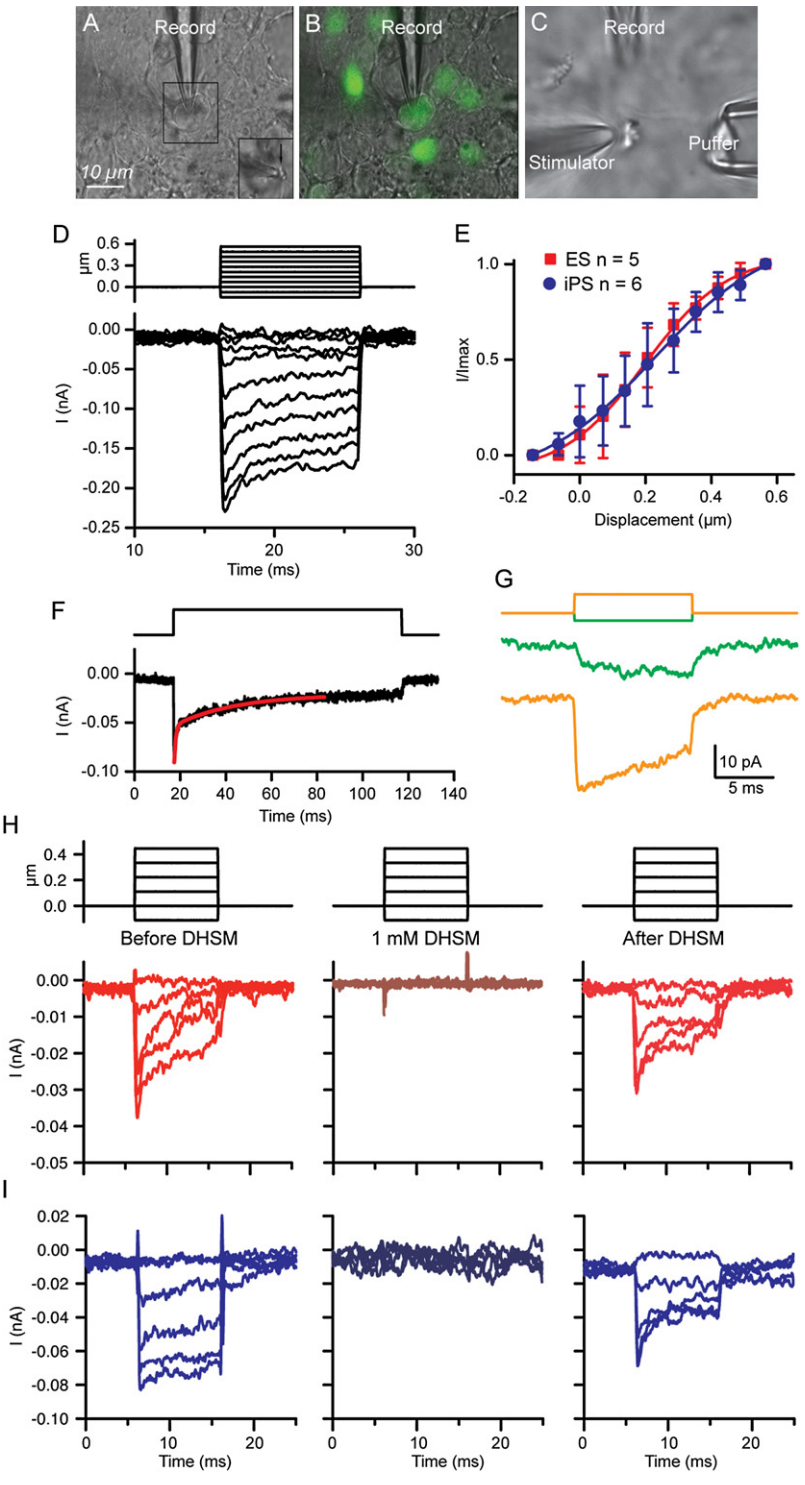

Figure 6. Mechanical Responses Elicited from ESC- and iPSC-Derived Bundle-Bearing Cells

(A–C) Experimental setup showing transmitted light image (A) with recording electrode on a cell of choice. The inset shows same cell with stimulus probe attached. The arrow points to the bundle.

(B) Fluorescent overlay onto (A) showing that recorded cell was $nGFP^{Atoh1}$ positive.

(C) Typical recording arrangement showing placement of patch electrode, stimulating electrode, and apical perfusion puffer.

(D) Example of currents elicited from an iPSC-derived cell in response to a series of mechanical deflections (shown above). Currents increased with stimulus intensity.

(E) Normalized current displacement plots for ESC- and iPSC-derived cells showing no difference in either half activation or sensitivity (solid lines are fits with Boltzmann functions with $r^2 = 0.99$ for both; details in the main text); error bars represent the SD.

(F) The response to an intermediate displacement for an iPSC-derived cell showing a time course for adaptation best fit by a double exponential. The red line is fit with time constants of 0.89 and 16.7ms ($r^2 = 0.99$).

(G) An example of the lack of directional sensitivity exhibited by many of the cells, here shown for an ESC-derived cell. Mechanical deflections of opposite polarity, shown above, elicited inward currents.

(H) ESC-derived (red) and (I) iPSC-derived (blue) cells with mechanically evoked currents that were reversibly blocked by 1 mM dihydrostreptomycin (DHSM). Stimulus is shown above currents.

in clusters, displayed hair bundle-like protrusions, and were surrounded by cells that showed features of inner ear supporting cells. Upon mechanical stimulation of bundles, the cells responded with currents reminiscent of immature hair cell transduction currents. Other currents detected in the young hair cell-like cells were variable in type and size. This observation suggests that voltage-dependent currents that are diagnostic for specific mature hair cell subtypes develop independently from hair bundles and mechanoelectrical transduction. We found no substantial differences between ESCs and iPSCs with respect to their ability to differentiate along the otic lineage or their differentiated hair cell-like function.

Guidance of ESCs and iPSCs toward the Otic Lineage

Pluripotent cells were guided in a step-wise manner toward an otic fate. Exposure to bFGF or FGF3/10 revealed that embryoid body-derived cultures, which were treated with Dkk1, SIS3, and IGF-1, were substantially more responsive to otic inducers than cultures that were only treated with Dkk1 and SIS3. IGF-1 therefore seems to anteriorize the ectoderm that was generated during embryoid body formation, increasing the number of cells capable of responding to otic-inducing FGFs. This anteriorizing effect of IGF signaling was previously observed in developing *Xenopus* embryos (Pera et al., 2001), used to promote anterior development of ESCs (Lamba et al., 2006), and increased responsiveness of anterior ectoderm to otic induction was reported in chicken embryos (Groves and Bronner-Fraser, 2000). It is interesting that the same logic that we

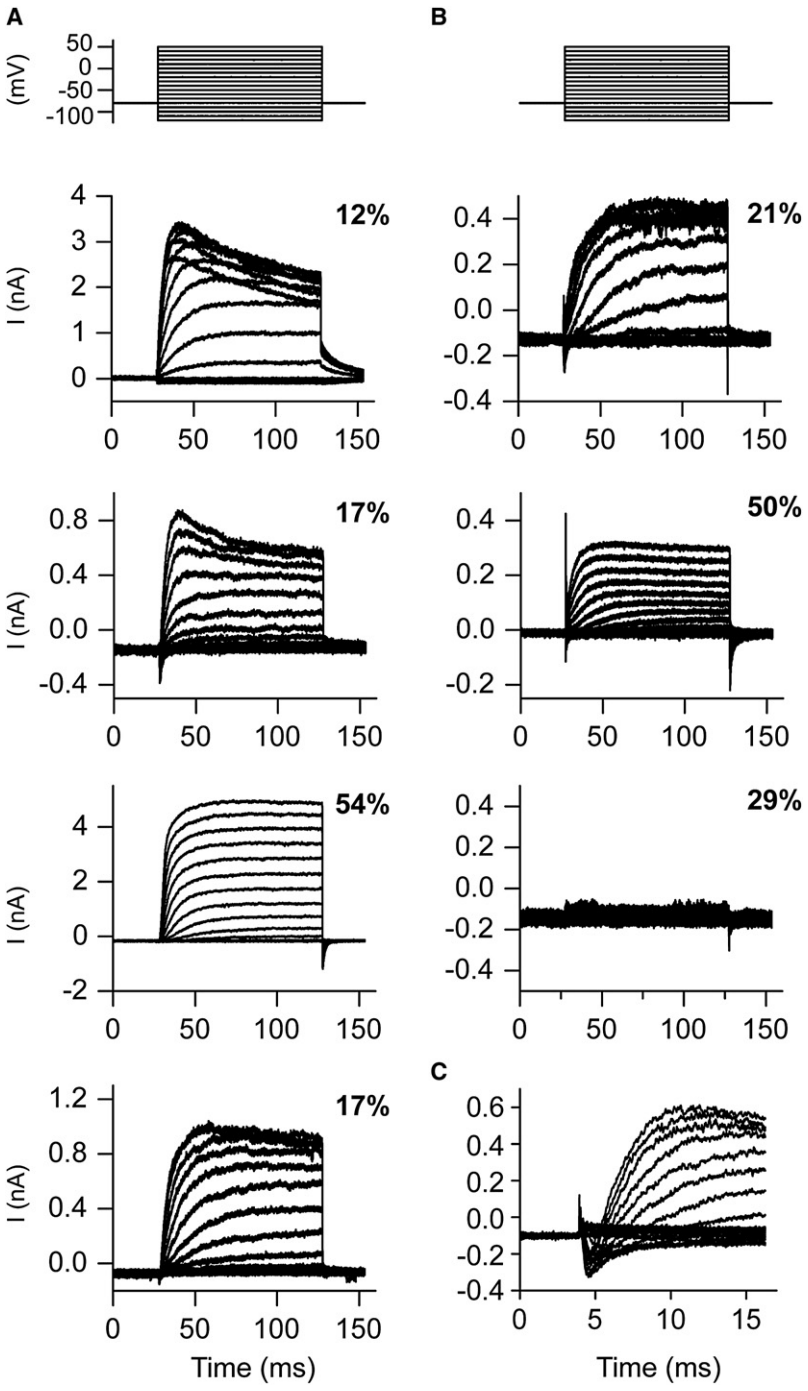

Figure 7. Voltage-Dependent Currents Elicited from ESC- and iPSC-Derived Bundle-Bearing Cells

(A and B) Green fluorescent cells derived from either ESCs or iPSCs were voltage clamped at −84 mV and stepped between −120 and 50 mV in 10 mV increments. The resultant complex current responses are shown in (A) when K^+ was in the internal solution and in (B) when Cs^+ was the major monovalent ion. The percentages reflect the proportion of cells with this basic response type. Inward currents were also observed in about 30% of the cells.

(C) Expanded view of the basic stimulus paradigm with Cs^+ internally is shown to highlight the inward component of the complex current.

applied to generate ectoderm that is responsive to inner ear inducers was utilized to guide ESCs toward retinal fate (Ikeda et al., 2005; Lamba et al., 2006; Osakada et al., 2008). In the case of retinal development, Pax6-positive precursors, often organized in neural rosettes, were observed. Our cultures also harbored Pax6-expressing cells that often occurred in rosettes (Figure S5C). These Pax6-positive cells were clearly distinct from the Pax2-expressing inner ear progenitor cells, indicating that retinal and otic lineages appeared to develop independently in D/S/I and bFGF-treated cultures.

Beside FGF signaling, activation of the canonical Wnt pathway has been proposed to further promote otic commitment of Pax2-expressing cells of the FGF-dependent pre-otic field of the chicken embryo (Ohyama et al., 2006). We did not observe an increase in the ability or efficiency of D/S/I and bFGF-treated cultures to generate hair cell-like cells when we supplemented the differentiation cultures with recombinant Wnt3a or LiCl (data not shown). An explanation for this result is that the cultures might already produce sufficient levels of Wnts. This speculation is supported by the observation that otic commitment, revealed by differentiation of hair cell marker-expressing cells, happens in the cultures without adding additional factors.

We previously have generated Pax2-expressing otic progenitors by using a protracted protocol that was based on selective survival of progenitors (Li et al., 2003). These cells were able to differentiate along the otic lineage after withdrawal of growth factors, and they displayed hair cell morphology when they were grafted into the developing inner ear of chicken embryos. In general, sensory cell types such as hair cell-like and photoreceptor-like cells generated by in vitro guidance of ESCs or, more recently, iPSCs (Hirami et al., 2009; Meyer et al., 2009) were characterized by immunocytochemistry. In-depth ultrastructural analysis of cytomorphological specializations and direct functional testing has not been applied to these cells. To test for these specializations and for function, we needed to determine culture conditions that promote the generation of hair bundles. Maintaining D/S/I and bFGF-treated ESCs and iPSCs on various substrates including fibronectin, gelatin, and MEF feeder cells confirmed that in vitro-generated otic progenitors are able to upregulate the hair cell marker myosin VIIa. Development of hair bundle-like structures and expression of hair bundle proteins

such as espin (Zheng et al., 2000), however, did not occur on these substrates. We hypothesized that the cells need additional signals and we tested whether expanded embryonic chicken utricle stromal cells would be able to provide such signals. Both ESC- and iPSC-derived otic progenitor cell cultures responded to stromal cells by organizing into clusters that were reminiscent of inner ear sensory epithelia (Figure S7). Experiments with stomal cell conditioned medium and coculture with fixed stromal cells indicate that the hair bundle-inducing activity is not present in conditioned media and that it is abolished by paraformaldehyde fixation. These results are compatible with a surface-linked and fixation-sensitive signal, but they do not exclude multiple factors or other more complex scenarios.

How Hair Cell-like Are ESC- and iPSC-Derived Hair Cell-like Cells?

Coculture with utricle stromal cells led to formation of F-actin-filled protrusions that were immunopositive for the hair bundle protein espin and single tubulin-filled kinocilia in cells that coexpressed myosin VIIa and $nGFP^{Atoh1}$. When we analyzed clusters of nGFP-positive cells by SEM, we found an organization of hair bundle-bearing hair cell-like cells surrounded by cells that displayed short microvilli, reminiscent of hair and supporting cells. Hair bundles displayed many other features, such as interciliary links, asymmetric stereciliary tops, and filamentous links from stereociliary tops to the neighboring stereocilia, tapering at the base, and immunoreactivity to antibodies to cadherin 23. Although the hair bundles were of various shapes, we did not detect typical mature cochlear bundle morphologies. The bundle morphologies appeared more generic, as if specificity had not yet been assigned.

Current responses obtained from mechanically stimulated bundles were similar to those obtained from immature hair cells where the currents were small, current-displacement functions were broad, the presence of adaptation and the rates measured were quite variable, and directional sensitivity was often absent (Lelli et al., 2009; Michalski et al., 2009; Waguespack et al., 2007). The time course of maturation of mechanotransduction varies depending both on end organ and on location within the end organ such that in mammalian cochlea basal cells mature 2–3 days earlier than apical outer hair cells. Mechanotransduction in basal outer hair cells begins at postnatal day 0. Vestibular hair cells mature in waves but begin neonatally around E16 (Géléoc and Holt, 2003). A common feature of the maturation is that the current amplitudes begin small, less than 100 pA; adaptation is nonexistent or slow, progressively becoming faster and more complete; and directional sensitivity is initially absent, becoming progressively more apparent (Waguespack et al., 2007). Maturation of the current responses takes about 5 days (Waguespack et al., 2007). Measurements presented here would suggest that mechanotransduction was within 2 days of the maturation process, with the variability in responses indicating a range of maturation of up to about 2 days.

Both the morphological and electrophysiological data suggest a common signaling pathway to trigger the development of a mechanosensitive hair bundle; however, additional signaling is required to specialize the bundle as well as to specify hair cell subtypes such as auditory or vestibular, inner or outer hair cell, or type I or type II hair cell. Supporting the argument that additional signaling is required to further specialize cells to specific phenotypic hair cells were the wide range of basolateral responses observed. The array of voltage-dependent currents measured suggest a distinct lack of appropriate signaling needed to promote complete maturation into specific hair cell subtypes. In both auditory and vestibular hair cells, there is a pattern of maturation where cells have a particular set of outward currents that include outward potassium (though limited selectivity) and inward sodium currents (Géléoc et al., 2004; Marcotti et al., 1999; Marcotti et al., 2003; Marcotti and Kros, 1999; Oliver et al., 1997). Both of these are transiently expressed and replaced by more selective channel types that vary depending on hair cell type and location within the end organ. Because of this diversity of channels, present data do not allow for the type of hair cell to be identified. As already pointed out, the lack of specificity in the basolateral conductances does suggest that hair bundle formation and development of mechanoelectrical transduction occurs independently of basolateral subtype specification.

Our findings provide a useful assay to study signals involved in hair cell subtype specification, a topic that is largely unexplored, particularly in mammals. Likewise, the guidance method outlined here offers a platform for molecular studies on hair cells, which are difficult to obtain in large numbers. A single retina, for example, harbors more than 120 million photoreceptors that can be isolated fairly easily, whereas a single mammalian inner ear only yields a few tens of thousand hair cells, which are difficult to dissect. The fact that in vitro-generated hair cell-like cells display mechanosensitivity demonstrated that generation of replacement hair cells from pluripotent stem cells is feasible, a finding that justifies the development of stem cell-based treatment strategies for hearing and balance disorders.

EXPERIMENTAL PROCEDURES

Cells and Culture

ESCs were isolated from blastocysts, and iPSCs were generated from fibroblasts of Math1/nGFP mice (Lumpkin et al., 2003). Details and culture procedures, including ectodermal guidance and otic induction are described in the Extended Experimental Procedures.

Marker Gene Expression Analysis

Cells were cultured in 4-well tissue culture plates (Greiner 35/10), harvested by lysis in the dish for RNA isolation, and RT-PCR or fixed and subjected to immunocytochemical analysis. Details are available in the Extended Experimental Procedures.

Statistical Analysis

Data are presented as mean values ± standard deviation (SD) with the number of independent experiments (n) indicated. Statistical differences were determined with paired two-tailed t tests using Aabel 3 (Gigawiz) on a Macintosh computer (Apple) running OS X.

Scanning Electron Microscopy

The cells were fixed for 2 hr with 2.5% glutaraldehyde/4% paraformaldehyde with 50 mM $CaCl_2$ and 20 mM $MgCl_2$ in 0.1 M HEPES buffer (pH = 7.4) and treated with 1% OsO_4 in the same buffer, 1% tannic acid in water, and 1% OsO_4 in water, followed by 1% tannic acid in water for 1 hr each. The specimens were washed three times between each treatment step and then dehydrated in a graded ethanol series, and finally dried by critical point drying.

Specimens were viewed with a Hitachi S-3400N variable pressure SEM operated under high vacuum at 5–10 kV at a working distance of 7–10 mm. All chemicals were supplied by Electron Microscopy Sciences (Hatfield, PA).

Hair Cell Mechanical Stimulation and Electrophysiology

nGFP-expressing hair cell-like cells were identified by fluorescence microscopy, and nearby hair bundle-like protrusions were imaged with a 100× objective with brightfield optics. Recordings were conducted with an Axoclamp 200a (Axon Instruments) amplifier, interfaced with a Digidata 1332 board (Axon), and jClamp Software (Scisoft). Mechanical stimulation was done with a stiff glass probe attached to a piezo stack. Details are described in the Extended Experimental Procedures.

SUPPLEMENTAL INFORMATION

Supplemental Information includes Extended Experimental Procedures and seven figures and can be found with this article online at doi:10.1016/j.cell.2010.03.035.

ACKNOWLEDGMENTS

We thank H. Zeng (Stanford Transgenic Research Center) for help with ESC line derivation; J. Johnson (UT Southwestern) for Math1/nGFP mice; U. Mueller (Scripps) for cadherin 23 antibody; G. Richardson for hair cell antigen antibody; F. Salles (National Institute on Deafness and Other Communication Disorders) for advice in electron microscopy sample preparation; L. Joubert (Stanford EM core facility) for expert assistance; M. Yazawa, R. Dolmetsch, and A. Ootani for help with teratoma assays; and K. Masaki, V. Starlinger, E. Corrales, M. Herget, Z. Guo, T. Jan, and S. Sinkkonen for fruitful discussions; M.D. is a fellow of the Alexander-von-Humboldt Foundation. This work was supported by National Institutes of Health grants DC006167 and P30DC010363, by the California Institute for Regenerative Medicine (grant RC1-00119-1), and by a Neuroscience of Brain Disorders Award from the McKnight Endowment Fund for Neuroscience.

Received: October 16, 2009
Revised: January 18, 2010
Accepted: February 24, 2010
Published: May 13, 2010

REFERENCES

Alsina, B., Abelló, G., Ulloa, E., Henrique, D., Pujades, C., and Giraldez, F. (2004). FGF signaling is required for determination of otic neuroblasts in the chick embryo. Dev. Biol. *267*, 119–134.

Azuara, V., Perry, P., Sauer, S., Spivakov, M., Jørgensen, H.F., John, R.M., Gouti, M., Casanova, M., Warnes, G., Merkenschlager, M., and Fisher, A.G. (2006). Chromatin signatures of pluripotent cell lines. Nat. Cell Biol. *8*, 532–538.

Beisel, K., Hansen, L., Soukup, G., and Fritzsch, B. (2008). Regenerating cochlear hair cells: quo vadis stem cell. Cell Tissue Res. *333*, 373–379.

Boëda, B., El-Amraoui, A., Bahloul, A., Goodyear, R., Daviet, L., Blanchard, S., Perfettini, I., Fath, K.R., Shorte, S., Reiners, J., et al. (2002). Myosin VIIa, harmonin and cadherin 23, three Usher I gene products that cooperate to shape the sensory hair cell bundle. EMBO J. *21*, 6689–6699.

Brigande, J.V., and Heller, S. (2009). Quo vadis, hair cell regeneration? Nat. Neurosci. *12*, 679–685.

Brown, S.T., Wang, J., and Groves, A.K. (2005). Dlx gene expression during chick inner ear development. J. Comp. Neurol. *483*, 48–65.

Chen, P., and Segil, N. (1999). p27(Kip1) links cell proliferation to morphogenesis in the developing organ of Corti. Development *126*, 1581–1590.

Diensthuber, M., Oshima, K., and Heller, S. (2009). Stem/progenitor cells derived from the cochlear sensory epithelium give rise to spheres with distinct morphologies and features. J. Assoc. Res. Otolaryngol. *10*, 173–190.

Eatock, R.A. (2000). Adaptation in hair cells. Annu. Rev. Neurosci. *23*, 285–314.

Forge, A., Li, L., Corwin, J.T., and Nevill, G. (1993). Ultrastructural evidence for hair cell regeneration in the mammalian inner ear. Science *259*, 1616–1619.

Freter, S., Muta, Y., Mak, S.S., Rinkwitz, S., and Ladher, R.K. (2008). Progressive restriction of otic fate: the role of FGF and Wnt in resolving inner ear potential. Development *135*, 3415–3424.

Gadue, P., Huber, T.L., Paddison, P.J., and Keller, G.M. (2006). Wnt and TGF-beta signaling are required for the induction of an in vitro model of primitive streak formation using embryonic stem cells. Proc. Natl. Acad. Sci. USA *103*, 16806–16811.

Géléoc, G.S., and Holt, J.R. (2003). Developmental acquisition of sensory transduction in hair cells of the mouse inner ear. Nat. Neurosci. *6*, 1019–1020.

Géléoc, G.S., Risner, J.R., and Holt, J.R. (2004). Developmental acquisition of voltage-dependent conductances and sensory signaling in hair cells of the embryonic mouse inner ear. J. Neurosci. *24*, 11148–11159.

Glinka, A., Wu, W., Delius, H., Monaghan, A.P., Blumenstock, C., and Niehrs, C. (1998). Dickkopf-1 is a member of a new family of secreted proteins and functions in head induction. Nature *391*, 357–362.

Goodyear, R.J., Legan, P.K., Wright, M.B., Marcotti, W., Oganesian, A., Coats, S.A., Booth, C.J., Kros, C.J., Seifert, R.A., Bowen-Pope, D.F., and Richardson, G.P. (2003). A receptor-like inositol lipid phosphatase is required for the maturation of developing cochlear hair bundles. J. Neurosci. *23*, 9208–9219.

Groves, A.K., and Bronner-Fraser, M. (2000). Competence, specification and commitment in otic placode induction. Development *127*, 3489–3499.

Hans, S., Liu, D., and Westerfield, M. (2004). Pax8 and Pax2a function synergistically in otic specification, downstream of the Foxi1 and Dlx3b transcription factors. Development *131*, 5091–5102.

Heller, N., and Brändli, A.W. (1999). Xenopus Pax-2/5/8 orthologues: novel insights into Pax gene evolution and identification of Pax-8 as the earliest marker for otic and pronephric cell lineages. Dev. Genet. *24*, 208–219.

Hirami, Y., Osakada, F., Takahashi, K., Okita, K., Yamanaka, S., Ikeda, H., Yoshimura, N., and Takahashi, M. (2009). Generation of retinal cells from mouse and human induced pluripotent stem cells. Neurosci. Lett. *458*, 126–131.

Hu, Z., and Corwin, J.T. (2007). Inner ear hair cells produced in vitro by a mesenchymal-to-epithelial transition. Proc. Natl. Acad. Sci. USA *104*, 16675–16680.

Ikeda, H., Osakada, F., Watanabe, K., Mizuseki, K., Haraguchi, T., Miyoshi, H., Kamiya, D., Honda, Y., Sasai, N., Yoshimura, N., et al. (2005). Generation of Rx+/Pax6+ neural retinal precursors from embryonic stem cells. Proc. Natl. Acad. Sci. USA *102*, 11331–11336.

Jinnin, M., Ihn, H., and Tamaki, K. (2006). Characterization of SIS3, a novel specific inhibitor of Smad3, and its effect on transforming growth factor-beta1-induced extracellular matrix expression. Mol. Pharmacol. *69*, 597–607.

Kazmierczak, P., Sakaguchi, H., Tokita, J., Wilson-Kubalek, E.M., Milligan, R.A., Müller, U., and Kachar, B. (2007). Cadherin 23 and protocadherin 15 interact to form tip-link filaments in sensory hair cells. Nature *449*, 87–91.

Kroese, A.B., Das, A., and Hudspeth, A.J. (1989). Blockage of the transduction channels of hair cells in the bullfrog's sacculus by aminoglycoside antibiotics. Hear. Res. *37*, 203–217.

Ladher, R.K., Wright, T.J., Moon, A.M., Mansour, S.L., and Schoenwolf, G.C. (2005). FGF8 initiates inner ear induction in chick and mouse. Genes Dev. *19*, 603–613.

Lamba, D.A., Karl, M.O., Ware, C.B., and Reh, T.A. (2006). Efficient generation of retinal progenitor cells from human embryonic stem cells. Proc. Natl. Acad. Sci. USA *103*, 12769–12774.

Lamba, D.A., Gust, J., and Reh, T.A. (2009). Transplantation of human embryonic stem cell-derived photoreceptors restores some visual function in Crx-deficient mice. Cell Stem Cell *4*, 73–79.

Lelli, A., Asai, Y., Forge, A., Holt, J.R., and Géléoc, G.S. (2009). Tonotopic gradient in the developmental acquisition of sensory transduction in outer hair cells of the mouse cochlea. J. Neurophysiol. *101*, 2961–2973.

Li, H., Roblin, G., Liu, H., and Heller, S. (2003). Generation of hair cells by stepwise differentiation of embryonic stem cells. Proc. Natl. Acad. Sci. USA *100*, 13495–13500.

Li, H., Liu, H., Corrales, C.E., Mutai, H., and Heller, S. (2004). Correlation of Pax-2 expression with cell proliferation in the developing chicken inner ear. J. Neurobiol. *60*, 61–70.

Lin, H.W., Schneider, M.E., and Kachar, B. (2005). When size matters: the dynamic regulation of stereocilia lengths. Curr. Opin. Cell Biol. *17*, 55–61.

Lumpkin, E.A., Collisson, T., Parab, P., Omer-Abdalla, A., Haeberle, H., Chen, P., Doetzlhofer, A., White, P., Groves, A., Segil, N., and Johnson, J.E. (2003). Math1-driven GFP expression in the developing nervous system of transgenic mice. Gene Expr. Patterns *3*, 389–395.

Marcotti, W., and Kros, C.J. (1999). Developmental expression of the potassium current IK,n contributes to maturation of mouse outer hair cells. J. Physiol. *520*, 653–660.

Marcotti, W., Géléoc, G.S., Lennan, G.W., and Kros, C.J. (1999). Transient expression of an inwardly rectifying potassium conductance in developing inner and outer hair cells along the mouse cochlea. Pflugers Arch. *439*, 113–122.

Marcotti, W., Johnson, S.L., Holley, M.C., and Kros, C.J. (2003). Developmental changes in the expression of potassium currents of embryonic, neonatal and mature mouse inner hair cells. J. Physiol. *548*, 383–400.

Marcotti, W., van Netten, S.M., and Kros, C.J. (2005). The aminoglycoside antibiotic dihydrostreptomycin rapidly enters mouse outer hair cells through the mechano-electrical transducer channels. J. Physiol. *567*, 505–521.

Martin, K., and Groves, A.K. (2006). Competence of cranial ectoderm to respond to Fgf signaling suggests a two-step model of otic placode induction. Development *133*, 877–887.

Meyer, J.S., Shearer, R.L., Capowski, E.E., Wright, L.S., Wallace, K.A., McMillan, E.L., Zhang, S.C., and Gamm, D.M. (2009). Modeling early retinal development with human embryonic and induced pluripotent stem cells. Proc. Natl. Acad. Sci. USA *106*, 16698–16703.

Michalski, N., Michel, V., Caberlotto, E., Lefèvre, G.M., van Aken, A.F., Tinevez, J.Y., Bizard, E., Houbron, C., Weil, D., Hardelin, J.P., et al. (2009). Harmonin-b, an actin-binding scaffold protein, is involved in the adaptation of mechanoelectrical transduction by sensory hair cells. Pflugers Arch. *459*, 115–130.

Michel, V., Goodyear, R.J., Weil, D., Marcotti, W., Perfettini, I., Wolfrum, U., Kros, C.J., Richardson, G.P., and Petit, C. (2005). Cadherin 23 is a component of the transient lateral links in the developing hair bundles of cochlear sensory cells. Dev. Biol. *280*, 281–294.

Ohyama, T., Mohamed, O.A., Taketo, M.M., Dufort, D., and Groves, A.K. (2006). Wnt signals mediate a fate decision between otic placode and epidermis. Development *133*, 865–875.

Oliver, D., Plinkert, P., Zenner, H.P., and Ruppersberg, J.P. (1997). Sodium current expression during postnatal development of rat outer hair cells. Pflugers Arch. *434*, 772–778.

Osakada, F., Ikeda, H., Mandai, M., Wataya, T., Watanabe, K., Yoshimura, N., Akaike, A., Akaike, A., Sasai, Y., and Takahashi, M. (2008). Toward the generation of rod and cone photoreceptors from mouse, monkey and human embryonic stem cells. Nat. Biotechnol. *26*, 215–224.

Oshima, K., Grimm, C.M., Corrales, C.E., Senn, P., Martinez Monedero, R., Géléoc, G.S., Edge, A., Holt, J.R., and Heller, S. (2007). Differential distribution of stem cells in the auditory and vestibular organs of the inner ear. J. Assoc. Res. Otolaryngol. *8*, 18–31.

Pauley, S., Wright, T.J., Pirvola, U., Ornitz, D., Beisel, K., and Fritzsch, B. (2003). Expression and function of FGF10 in mammalian inner ear development. Dev. Dyn. *227*, 203–215.

Pera, E.M., Wessely, O., Li, S.Y., and De Robertis, E.M. (2001). Neural and head induction by insulin-like growth factor signals. Dev. Cell *1*, 655–665.

Phillips, B.T., Storch, E.M., Lekven, A.C., and Riley, B.B. (2004). A direct role for Fgf but not Wnt in otic placode induction. Development *131*, 923–931.

Pirvola, U., Spencer-Dene, B., Xing-Qun, L., Kettunen, P., Thesleff, I., Fritzsch, B., Dickson, C., and Ylikoski, J. (2000). FGF/FGFR-2(IIIb) signaling is essential for inner ear morphogenesis. J. Neurosci. *20*, 6125–6134.

Pirvola, U., Ylikoski, J., Trokovic, R., Hébert, J.M., McConnell, S.K., and Partanen, J. (2002). FGFR1 is required for the development of the auditory sensory epithelium. Neuron *35*, 671–680.

Ricci, A. (2002). Differences in mechano-transducer channel kinetics underlie tonotopic distribution of fast adaptation in auditory hair cells. J. Neurophysiol. *87*, 1738–1748.

Rowitch, D.H., and McMahon, A.P. (1995). Pax-2 expression in the murine neural plate precedes and encompasses the expression domains of Wnt-1 and En-1. Mech. Dev. *52*, 3–8.

Siemens, J., Lillo, C., Dumont, R.A., Reynolds, A., Williams, D.S., Gillespie, P.G., and Müller, U. (2004). Cadherin 23 is a component of the tip link in hair-cell stereocilia. Nature *428*, 950–955.

Takahashi, K., and Yamanaka, S. (2006). Induction of pluripotent stem cells from mouse embryonic and adult fibroblast cultures by defined factors. Cell *126*, 663–676.

Tilney, L.G., Egelman, E.H., DeRosier, D.J., and Saunder, J.C. (1983). Actin filaments, stereocilia, and hair cells of the bird cochlea. II. Packing of actin filaments in the stereocilia and in the cuticular plate and what happens to the organization when the stereocilia are bent. J. Cell Biol. *96*, 822–834.

Tilney, L.G., Tilney, M.S., and DeRosier, D.J. (1992). Actin filaments, stereocilia, and hair cells: how cells count and measure. Annu. Rev. Cell Biol. *8*, 257–274.

Vendrell, V., Carnicero, E., Giraldez, F., Alonso, M.T., and Schimmang, T. (2000). Induction of inner ear fate by FGF3. Development *127*, 2011–2019.

Waguespack, J., Salles, F.T., Kachar, B., and Ricci, A.J. (2007). Stepwise morphological and functional maturation of mechanotransduction in rat outer hair cells. J. Neurosci. *27*, 13890–13902.

Warchol, M.E., Lambert, P.R., Goldstein, B.J., Forge, A., and Corwin, J.T. (1993). Regenerative proliferation in inner ear sensory epithelia from adult guinea pigs and humans. Science *259*, 1619–1622.

Wright, T.J., and Mansour, S.L. (2003). Fgf3 and Fgf10 are required for mouse otic placode induction. Development *130*, 3379–3390.

Wu, Y.C., Ricci, A.J., and Fettiplace, R. (1999). Two components of transducer adaptation in auditory hair cells. J. Neurophysiol. *82*, 2171–2181.

Xu, P.X., Adams, J., Peters, H., Brown, M.C., Heaney, S., and Maas, R. (1999). Eya1-deficient mice lack ears and kidneys and show abnormal apoptosis of organ primordia. Nat. Genet. *23*, 113–117.

Zheng, L., Sekerková, G., Vranich, K., Tilney, L.G., Mugnaini, E., and Bartles, J.R. (2000). The deaf jerker mouse has a mutation in the gene encoding the espin actin-bundling proteins of hair cell stereocilia and lacks espins. Cell *102*, 377–385.

Zou, D., Silvius, D., Fritzsch, B., and Xu, P.X. (2004). Eya1 and Six1 are essential for early steps of sensory neurogenesis in mammalian cranial placodes. Development *131*, 5561–5572.